Evaluation of the strength of slender pillars

G.S. Esterhuizen
Mining Engineer, National Institute for Occupational Safety and Health, Pittsburgh, Pennsylvania

Abstract

Pillars with width-to-height ratios of less than 1.0 are frequently created in underground hard rock mines. The strength of slender pillars can be estimated using empirically developed equations. However, the equations can provide variable results when the width-to-height ratios approach 0.5. This paper investigates some of the issues affecting pillar strength at low width-to-height ratios in hard brittle rock. The investigation includes an evaluation of empirical pillar strength data presented in the literature and observations of pillar performance in underground limestone mines in the eastern United States, supplemented by numerical modeling in which failure processes and sensitivity of slender pillars to variations in rock mass properties are evaluated. The results showed that the strength of slender pillars is more variable than that of wider pillars. The numerical model results demonstrated the increasing role of brittle rock failure in slender pillar strength. The absence of confinement in slender pillars can result in a fully brittle failure process, while wider pillars fail in a combined brittle and shearing mode. The onset of spalling in slender pillars occurs at or near the ultimate strength, while this is not the case for wider pillars. Slender pillars are shown to be more sensitive to the presence of discontinuities than wider pillars, which can partly explain the increased variability of slender pillar strength. Two examples are presented that illustrate failure initiation by brittle spalling and the sensitivity of slender pillars to the presence of discontinuities.

Introduction

The National Institute for Occupational Safety and Health's (NIOSH's) Pittsburgh Research Laboratory has embarked on a project to develop pillar design guidelines for underground limestone mines. A survey of mining methods and pillar and room dimensions in 70 underground limestone mines (Iannacchione, 1999) showed that the room-and-pillar method was used in 69 of the 70 mines surveyed. The average depth of cover was 80 m (260 ft), varying between 7 m (23 ft) and 610 m (2,000 ft). Pillars were typically square in plan view, but rectangular or rib pillars are also used. During initial development, the average pillar width-to-height (w:h) ratio was 1.73 but was reduced to 0.92 after bench mining of the floor. The minimum and maximum w:h ratio observed in the study was 0.4 and 3.13, respectively. Nine cases of pillar failure were identified, with all of them at width-to-height ratios of less than or equal to 1.5. Because floor benching is conducted in more than half of the limestone mines, pillars that were previously stable could become unstable when their width-to-height ratio is reduced during benching. NIOSH has, therefore, initially focused the project on the strength of slender pillars.

The design of stable pillars requires that both the strength and loading of the pillars be known. In addition, an appropriate safety factor should be selected to ensure that the variability and uncertainty of the pillar strength and loading is accounted for. In the case of regular arrays of flat lying pillars, the load can be estimated by the tributary area method (Salamon and Munro, 1967), or if the layout is more complex, estimates of average pillar loading can be obtained from numerical models (Brady and Brown, 1985).

Pillar strength can be estimated from empirical equations that have been developed by observing both failed and stable pillar configurations. The pioneering work in this field was carried out for coal mine pillar design (Salamon and Munro, 1967; Bieniawski and van Heerden, 1975). Several empirically based pillar strength equations have since been developed for hard rock mines (Hedley and Grant, 1972; von Kimmelman et al. (1984); Lunder and Pakalnis, 1997).

Analytical methods to estimate pillar strength have been developed, such as Wilson's confined core model (Wilson, 1972) and a similar model by Barron (1986). Although these methods have assisted in understanding pillar failure mechanics, they have not found wide acceptance as design tools in the mining industry.

More recently, numerical models have found increasing use in pillar design (Mark, 1999). For example, Hoek and Brown (1980) used the results of elastic models to estimate the strength of pillars in various rock-mass classes. Martin and

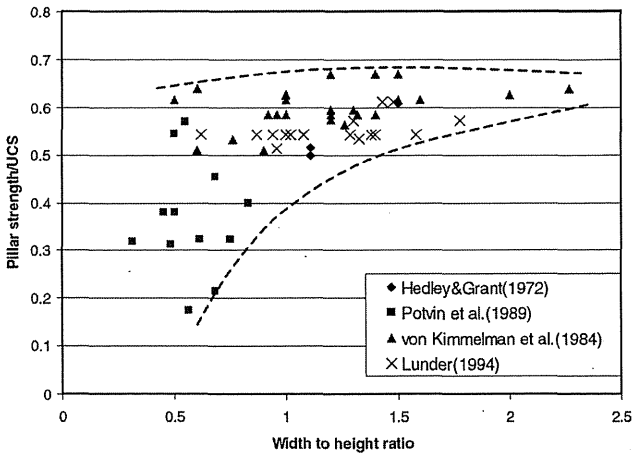

Figure 1 — Pillar stability graph showing published case histories of failed pillars from hard rock metal mines.

Maybee (2000) used elastic models to evaluate the effect of brittle failure on hard-rock pillars, while Lunder and Pakalnis (1997) used numerical model results to assist in developing an empirically based pillar strength equation for hard-rock mines. Numerical models have been used to assess geological effects such as through-going joints and weak floor on pillar strength (Gale, 1999; Iannacchione, 1999; Esterhuizen, 2000). Models that simulate rock fracture and elemental particulate behavior show promise in developing more realistic simulations of pillar failure mechanics (Diederichs, 2002; Elmo et al., 2005). The role of numerical modeling in pillar design is now well established and has assisted in developing new approaches to pillar stability assessment and design, such as the development of a semi-empirical hazard-prediction system for pillars and stopes in a deep Canadian mine (Diederichs et al., 2002).

Owing to the limited cases of pillar failure in underground limestone mines, purely empirical methods that rely on the study of pillar failures have limited application. NIOSH is, therefore, following an approach that combines empirical observations and numerical models to develop a pillar design methodology for underground limestone mines. This paper presents the results of an evaluation of slender pillar strength through a review of empirical pillar design methods for hard rock mines, observation of pillar performance in limestone mines and numerical model analysis of slender pillars. Two examples of slender pillar instability in limestone mines are presented and discussed.

For the purpose of this paper, pillars with width-to-height ratios of less than 1.0 are called slender pillars. Pillar strength is defined as the peak load-bearing capacity per unit area of a pillar. A pillar is considered to be failed if it is compressed beyond its strength and sheds load. During underground observations it can be difficult to visually assess whether a pillar has failed or not, because rock failure might be observed around the perimeter of the pillar, but the pillar as a whole may not have reached its peak resistance.

Slender pillars in empirical studies

Case histories of pillar failure from a number of empirical studies (Hedley and Grant, 1972; van Kimmelman et al., 1984; Potvin et al., 1989; Lunder, 1994) are summarized in Fig. 1, which represents the pillar strength as a function of the width-to-height ratio. The pillar strength is normalized by the uniaxial compressive strength (UCS) of the rock material. The graph also shows the upper and lower bounds of the failed cases.

The empirical studies were all carried out at metal mines with good- to very good-quality rock masses (RMR 60-85). Pillar failure was determined by visual inspection in all cases, and pillar loads were estimated by the tributary area method or through numerical modeling. None of the failed pillars were affected by major structures such as faults, so that the pillar stability was reflective of the general rock mass behavior. It can be seen that slender pillars are well represented by the case histories.

Variability of failure strength of case histories. Figure 1 clearly shows that, for the presented case histories, the pillar strength becomes highly variable as the width-to-height ratio decreases. The standard deviation of the strengths of slender pillars is 25.4%, while it is 7.8% for the wider pillars. The variability can be caused by several factors, which can include uncertainty of the actual rock strength, uncertainty of the pillar stress, variations in the degree and severity of jointing, a variation in the bedding characteristics and the presence of weak bands in the pillars.

The uncertainty and variability of pillar strength and loading is accounted for in pillar design by selecting an appropriate safety factor. The safety factor is the ratio of the average pillar strength to average pillar load. If pillar strength or loads are highly variable, a larger safety factor is required to account for the increased variability. The objective when selecting a safety factor is to limit the failure probability of the pillars to some acceptable level. For example, a safety factor of 1.6 is commonly used for pillar design in South Africa, achieving a failure probability of less than 0.5% (Wagner, 1992).

The high variability of slender pillar strength, seen in the case history database, implies that slender pillars require a higher safety factor than wider pillars.

Empirical equations and slender pillar strength. A review of the empirically developed pillar strength equations for hard rock mines reveals that the equations can be placed into three groups:

- *Power equations:* Power equations such as the Hedley and Grant (1972) equation used in hard rock pillar design

$$S = k\frac{w^{0.5}}{h^{0.75}} \qquad (1)$$

where
k is the strength of a unit cube of the rock material forming the pillar,
w is the pillar width and
h is the height of the pillar.

This equation follows the form of the coal pillar strength equation developed by Salamon and Munro (1967).

- *Linear equations:* Linear equations, such as the equation originally proposed by Obert and Duvall (1967) based on laboratory tests on rock samples

$$S = \sigma_p(0.778 + 0.222\frac{w}{h}) \qquad (2)$$

where
σ_p is the strength of a pillar with a width-to-height ratio of 1.0.

- *Equation based on pillar confinement:* An equation based on pillar confinement was developed by Lunder and Pakalnis (1997)

$$S = (K * UCS)(C_1 + \kappa C_2) \quad (3)$$

where
κ is a pillar friction term,
C_1 and C_2 are empirically derived constants determined to be 0.68 and 0.52, respectively, and
K is the rock mass strength size factor, determined to be 0.44.

The value of κ can be determined by

$$\kappa = \tan\left[\cos^{-1}\left(\frac{1-Cpav}{1+Cpav}\right)\right] \quad (4)$$

where
$Cpav$ is the average pillar confinement, which can be found by

$$Cpav = 0.46\left[\log\left(\frac{W_p}{h} + 0.75\right)\right]^{\frac{1.4}{W_p/h}} \quad (5)$$

where
W_p is the pillar width and
h is the pillar height.

These three forms of equations were compared by entering similar rock strength parameters in each. This was achieved by setting the large-scale strength of the rock mass (k) equal to 0.42 times the UCS in the Hedley–Grant equation and similarly setting the value of σ_p in the Obert-Duval equation. The result is shown in Fig. 2. Comparing the three curves shows that the Hedely-Grant and the Lunder-Pakalnis equations predict similar pillar strengths when the w:h ratio exceeds 0.6, but they diverge at lower w:h ratios.

Interestingly, the Lunder-Pakalnis equation predicts constant pillar strength below w:h ratios of 0.4. The Obert-Duval equation is linear and predicts higher strength for slender pillars than the other two equations. For example, the Obert-Duval equation predicts a strength of 0.38 times the UCS for a pillar with a w:h ratio of 0.5, while the Hedley-Grant equation predicts 0.30 and the Lunder-Pakalnis equation predicts 0.31. There is a difference of 26% between the highest and the lowest predictions.

The review shows that the three forms of pillar strength equations considered will result in significantly different estimates of slender pillar strength for the same rock mass strength data. The equations also predict different trends in strength, especially at low width to height ratios. When designing slender pillars, the selection of a strength equation can, therefore, have a significant impact on the resulting dimensions of slender pillars. The numerical modeling discussed in this paper was carried out partly to evaluate pillar strength issues at low w:h ratios.

Pillar failure in hard rock mines

Pillar failure modes in hard rock mines can be divided into two categories (Iannacchione, 1999). The first category is failure of the rock mass, in which spalling or crushing occurs through the intact rock and shearing occurs along natural joint planes in the rock. This failure mode is progressive and can be described in the following stages, after Krauland and Soder (1987):

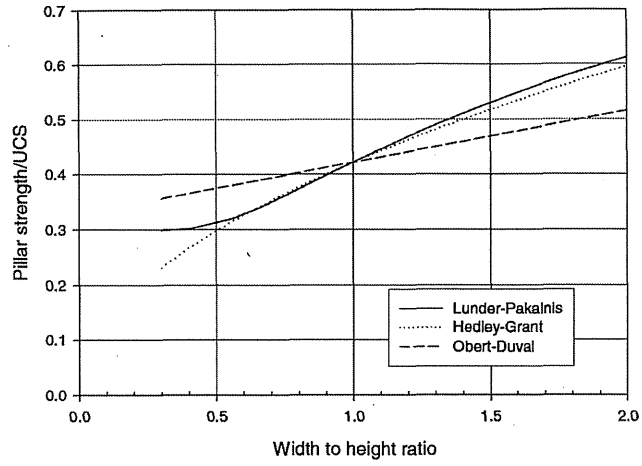

Figure 2 — Comparison of pillar strength equations.

- *Stage 1:* slight spalling of pillar corners and walls;
- *Stage 2:* severe spalling;
- *Stage 3:* the appearance of fractures in the central part of the pillar;
- *Stage 4:* the occurrence of rock falls from the pillar, emergence of an hourglass shape; and
- *Stage 5:* the disintegration of the pillar or, alternatively, the formation of a well-developed hourglass with the central parts completely crushed.

In this category of failure, brittle spalling occurs initially through the intact rock, followed by shearing and crushing of the rock mass. The initial brittle failure appears to be independent of the natural joints and bedding planes in strong rock (Diederichs et al., 2002; Diederichs, 2002).

The second category of failure is structure controlled, where shearing occurs along an individual geological structure such as a through-going joint or fault. Other modes of structural failure can occur when weak bedding layers or soft joint fill exists in a pillar that can extrude and destroy the pillar by inducing tension in the surrounding rock. Sliding along weak roof or floor contacts can induce similar failure modes in a pillar and is classified under the structural failure mode.

Assessment of slender pillar strength using numerical models

Numerical models were used to further investigate the strength of slender pillars and to address some of the issues related to the pillar strength equations. The FLAC3D (Anon., 2002) finite difference software was used to conduct the modeling. The software has the capability to model elastic and strain softening behavior using an elasto-plastic constitutive law. Important to this project was for the models to replicate realistically the failure processes observed in hard rock pillars.

Modeling brittle rock mass failure. It is important that the two-stage process of brittle spalling followed by shearing should be replicated in the numerical models. The phenomenon of brittle spalling has received much attention in the rock mechanics literature in recent years (Kaiser et al. 2000; Martin and Maybee, 2000, Rojat et al., 2003). It has been found that the onset of brittle spalling typically occurs at 0.3 to 0.5 the uniaxial compressive strength of the rock, which is the stress level required for crack initiation. Stacey and Yathavan (2003)

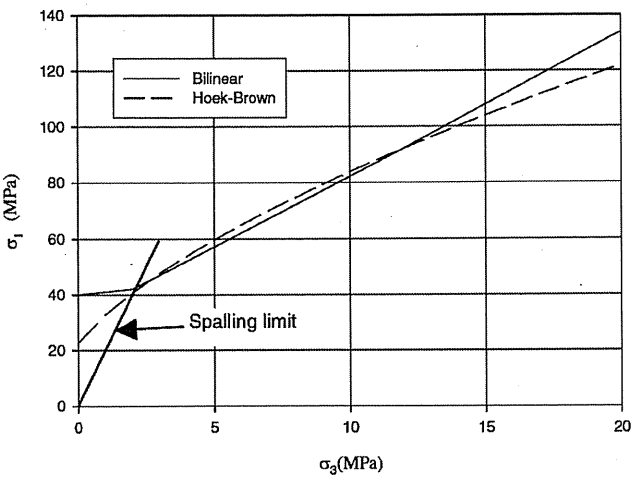

Figure 3 — Bilinear and Hoek-Brown (1980) rock-strength plots for a rock mass rating of 70.0.

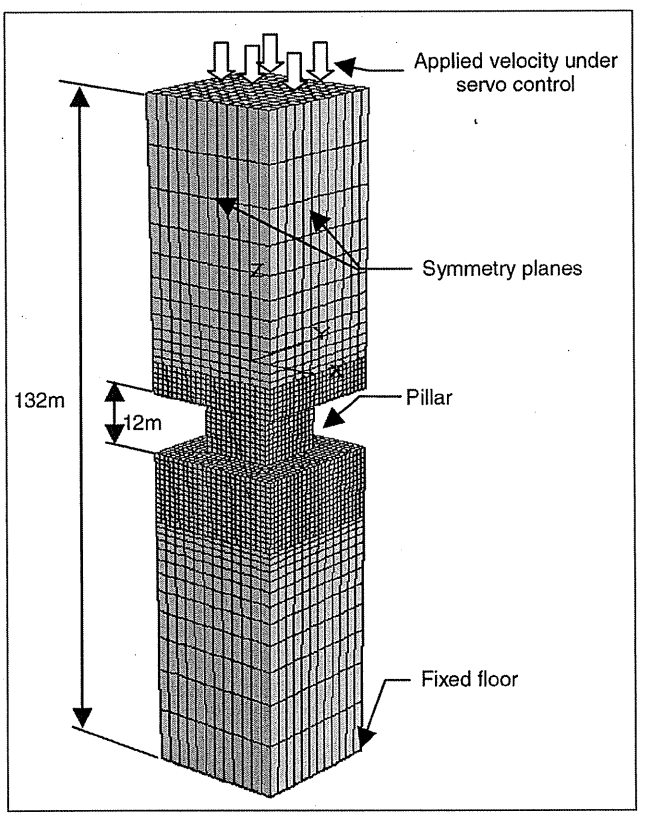

Figure 4 — Model used to simulate a pillar in FLAC3D.

presented a number of cases in which brittle spalling occurred below 0.2 times the UCS and possibly as low as 0.04 in one case. The brittle cracks typically extend and develop into fractures that are parallel to the major principal stress. According to Kaiser et al. (2000), at low confinement, stresses crack dilation inhibits the mobilization of frictional resistance until the rock is sufficiently damaged. They proposed a bilinear strength envelope for rock around underground openings in which the strength at low confinement is independent of friction and is equal to 0.3 to 0.5 times the UCS, followed by friction hardening at higher confinement, increasing up to the strength predicted by the Hoek-Brown (1997) or similar rock strength criteria. The change from brittle spalling to frictional resistance occurs at a ratio of the maximum to minimum principal stress of 10 to 20, which depends on the heterogeneity and jointing in the rock mass.

The FLAC3D software has a built-in constitutive model for bilinear rock strength based on the Mohr-Coulomb strength criterion, in which strain hardening or softening is a function of the deviatoric plastic strain (Anon., 2002). This model can include ubiquitous joints that can be used to evaluate the effect of through-going joint sets on rock mass strength. The bilinear model is well suited to simulate the brittle/frictional development of rock mass strength as a function of confining stress. The initial brittle strength was based on the assumptions that spalling initiates at 0.33 times the UCS, and the transition from brittle to frictional strength occurs when the ratio of maximum to minimum principal stress (σ_1/σ_3) is 20.0. For the brittle section of the strength curve, the friction value was set to zero, after Martin and Maybee (2000). The parameters for the fully developed frictional rock-mass strength were based on the Hoek-Brown (1997) criterion by approximating the predicted rock mass strength with appropriate Mohr-Coulomb parameters.

Figure 3 shows the Hoek-Brown (1997) strength curve and the approximate bilinear strength curve for a rock mass rating (RMR) of 70, a UCS of 120 MPa (17,400 psi) and Hoek-Brown (1997) m-parameter of 12.0, which simulates a good-quality rock mass.

The strain softening parameters for the models were determined as part of the model-calibration process because they are affected by model element size (Anon., 2002). All the models were run using identical element sizes.

Modeling of structure controlled failure. The effect of through-going joints was modeled using the ubiquitous joint facility of the bilinear constitutive model in FLAC3D. The software allows joint sets to be defined in each model element having a specific orientation and Coulomb strength parameters. During the analysis of the effect of structure controlled failure, the rock mass maintained its brittle characteristics through the bilinear constitutive model.

Model geometry and loading conditions. The models were set up to simulate a single pillar with the adjacent roof and floor rocks, as shown in Fig. 4. Both the pillar width and room width were set to 12 m, resulting in 75% extraction. The height of the pillar was varied to simulate different width-to-height ratios. Vertical symmetry planes were defined to coincide with the vertical sides of the model, simulating a repeating system of rooms and pillars. Owing to symmetry, only half of the width of the rooms was included in the models. The floor of the models was fixed in the vertical direction. The top surface of the model was subject to an applied downward velocity that simulated crushing of the pillar under increased compression. The applied velocity was subject to servo control to maintain the unbalanced forces in the model within acceptable levels (Anon., 2002).

The models were run to equilibrium under elastic conditions subject to a vertical field stress of 2.7 MPa (390 psi), simulating a mine at 100 m (328 ft) depth. The horizontal stress was also set at 2.7 MPa (390 psi). After reaching equilibrium in the elastic state, the pillar material was changed from elastic to the bilinear Mohr-Coulomb material type. The model was then subject to increasing vertical loading by applying the servo-controlled

velocities at the top of the model. The models were compressed until the pillar had completely failed and had reached a residual strength of less than 50% of the peak strength.

During the simulations the average vertical stress at mid-height of the pillar was calculated at regular intervals. The peak value of this stress was considered to represent the pillar strength. In addition, the closure between the top and bottom of the pillar was recorded, so that a pillar stress–strain curve could be developed. A routine was developed using the internal programming language available in FLAC3D, which recorded whether failure of an element occurred during the initial brittle stage or the shearing stage of the strength curve.

Model calibration and testing. Model calibration was carried out by simulating pillars with w:h ratios of 0.3, 0.4, 0.66, 0.8, 1.0, 1.5 and 2.0 and comparing the results to the Lunder-Pakalnis (1997), empirically developed pillar strength equation. The models were all set up to simulate a good-quality rock mass with an RMR value of 70. This value of RMR is in the center of the range of RMR values of 60 to 80 reported for the case histories used by Lunder and Pakalnis (1997) to develop the strength equation. Details of the input data for this model are presented in Table 1.

The calibration was carried out by varying the rate of cohesion softening in the models and keeping all the other parameters constant. Figure 5 shows the final result of the calibration runs. As shown, the model results predict a flattening of the strength curve at low w:h ratios similar to the Lunder-Pakalnis (1997) curve.

The sensitivity of the models to the rock strength parameters was tested by varying the rock-mass strength parameters to simulate RMR values of 60 to 80. This was achieved by modifying the uniaxial compressive strength as well as the cohesion and friction values in accordance with the Hoek-Brown (1997) strength criterion. The spalling limit was maintained at 30% of the UCS in all the models. The results are presented in Fig. 6, which shows that a reduction in the RMR to 60 does not have a significant effect on the pillar strength, while an increase to RMR = 80 results in a rapid increase in the strength of wider pillars. In all cases, the strength of pillars with w:h of 0.8 and less was equal to the brittle strength of the rock. All the model runs described below were carried out using the rock mass strength parameters for an RMR value of 70, as shown in Table 1.

Pillar failure modes derived from model results. Inspection of the extent of brittle failure and shearing failure in the models showed that the pillars with w:h ratios of 0.8 and below fail in the brittle mode, owing to the absence of sufficient confinement in these pillars to mobilize the frictional component of the rock strength. This explains the flattening of the pillar strength curve to the brittle rock strength seen in Fig. 6. The extent of brittle and shear failure in pillars with w:h ratios of 0.5, 1.0 and 2.0 are presented in Fig. 7, illustrating the increasing role of brittle failure as the w:h ratio decreases.

Failure of the wider model pillars initiates by brittle failure around the outside of the pillar, which commences when the stress in the outer skin of the pillar exceeds the brittle rock strength. The brittle failure process continues as the pillar load increases. As the pillar approaches its peak strength, shear failure starts to develop behind the brittle failure zone. The pillar load can start to decrease before shear failure has progressed to the pillar core. This type of behavior is similar to the results of compression tests on small coal pillars reported by Wagner (1974).

Table 1 — Input parameters for the RMR = 70 model.

Parameter	Value
Elastic modulus	70 GPa (1x10^7 psi)
Poisson ratio	0.2
Intact rock strength (UCS)	120 MPa (17,400 psi)
First stage (brittle) cohesion	20 MPa (2,900 psi)
First stage (brittle) friction angle	0°
Second stage cohesion	6.5 MPa (940 psi)
Second stage friction angle	42.7°
Tensile strength	7 MPa (1,000 psi)
Dilation angle	30°

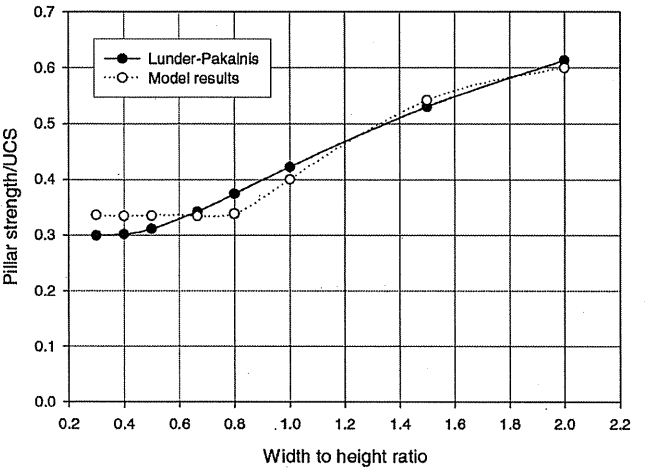

Figure 5 — Results of model calibration against the Lunder-Pakalnis (1997) empirically derived pillar-strength equation.

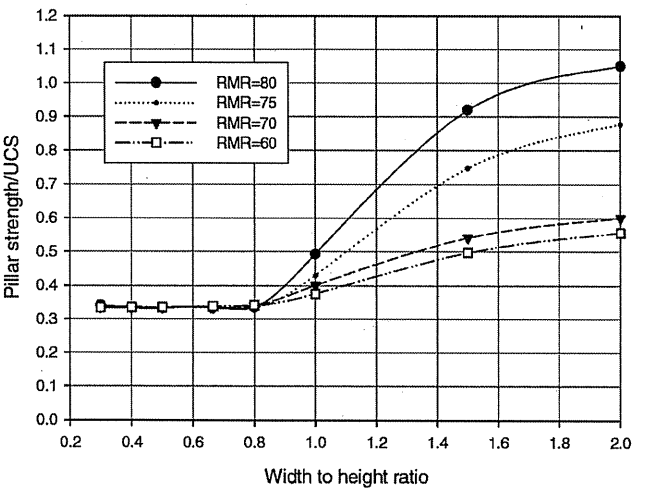

Figure 6—Effect of rock mass rating (RMR) on pillar strength determined from numerical model results.

Slender pillars with w:h ratios of 0.8 and less also start to fail by brittle spalling when the average pillar stress approaches the brittle rock strength. However, a small increase in load results in failure of the entire pillar followed by rapid load shedding. In these slender models, brittle failure did not always com-

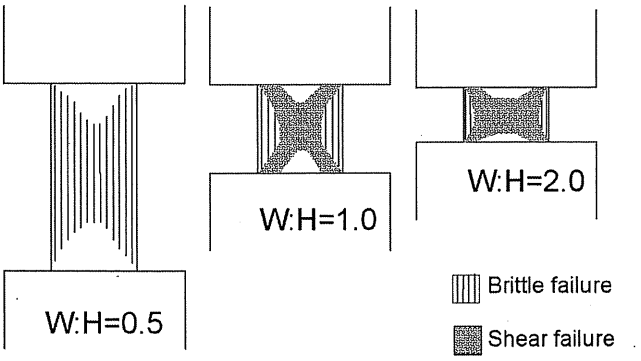

Figure 7 — Sections through the center of pillars with different width to height ratios showing the extent of brittle and shear failure of the rock mass predicted by numerical modeling.

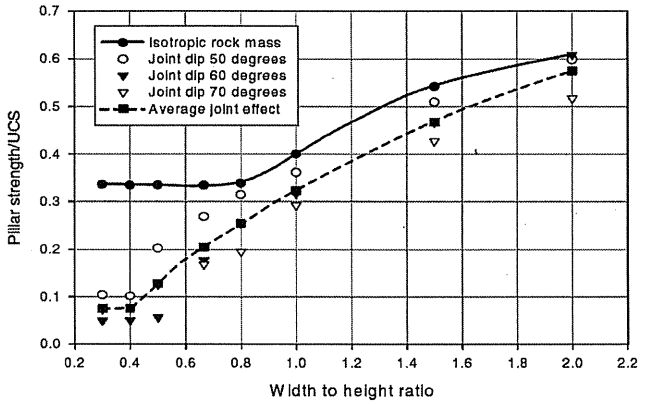

Figure 8 — Numerical model results of pillar strength vs. width-to-height ratio, showing the effect of discontinuities inclined at 50° to 70° on pillar strength.

mence at the outer skin of the pillar, but could start near the pillar center. According to the model results, pillars with w:h ratios of 0.8 or less will be at or near their ultimate strength when they start to show signs of brittle failure.

Model results of the effect of inclined discontinuities. The strength parameters used in the models discussed above are based on the assumption that the rock-mass strength is isotropic, implying that the discontinuity orientations and spacings are also isotropic. In practice, one of the discontinuity sets can be dominant and will result in anisotropic strength in the rock mass. To investigate the effect of a single dominant discontinuity set on pillar strength, the ubiquitous joint facility in FLAC3D was used. A single discontinuity set, striking parallel to one of the pillar sides, was introduced into the pillar models. The discontinuity dip was varied from 50° to 70° in each model. The discontinuity strength was selected to simulate rough joints with unaltered joint walls that are continuous relative to the pillar dimensions. The Coulomb parameters used for these discontinuities were determined using the approach of Barton and Choubey (1997). The strength parameters were Cohesion = 1.2 MPa (170 psi) and friction angle = 42°.

The results are summarized in Fig. 8, which shows that the presence of the inclined discontinuities can have a significant effect on the strength of slender pillars, while the wider pillars are affected to a much lesser degree. For example, discontinuities dipping at 70° reduce the strength of a pillar with w:h ratio of 2.0 by 13%, while the strength of a pillar with a w:h ratio of 0.5 is reduced by 62%.

Examples of slender pillar performance

Observations of pillars in underground limestone mines have revealed most of the characteristics of slender pillar failure described above. Presented below are two examples, one presents brittle spalling at low stress and the other shows the effect of through-going discontinuities.

Example of brittle spalling. Brittle spalling and hourglass formation at relatively low stress was observed at a mine in northern Tennessee that uses the room-and-pillar method. In the area of concern, the pillars were square with side dimensions varying from 12.2 to 15.2 m (40 to 50 ft) and were developed about 15.8 m (52 ft) high. Benching was partially carried out, which increased the pillar height to 21 m (70 ft). The room width was measured to be 16.4 m (53 ft), and the depth of cover was 140 m (464 ft).

The limestone is a strong rock mass with a UCS of 150 MPa (22,000 psi). Jointing is near vertical with an average spacing of about 0.5 m (1.6 ft). Joint surfaces are rough, and the joint continuity is less than 3 m (10 ft). Bedding joints are poorly developed and did not appear to affect the pillar stability.

The pillars were about 15 years old and were reported to be progressively spalling to an hourglass shape, as shown in Fig. 9. Based on visual observations, it is not certain whether these pillars had failed. Inspection of the pillars revealed that open vertical fractures or joints could be seen in the pillar ribs. Columnar fragments of rock about 2 m (6.6 ft) long were scattered about the pillars, as seen in the foreground. The average pillar stress, calculated by the tributary area method, is 15 MPa (2,175 psi), which is only 10% of the UCS of the intact rock. This is at the lower end of the range of observed cases of brittle spalling. The presence of near-vertical open fractures and joints seems to confirm that a brittle failure process is taking place in these pillars.

Example of the effect of inclined discontinuities. The second case is a limestone mine in western Pennsylvania that uses the room-and-pillar method of mining. The limestone is massive and is fine to medium grained with cross bedding. Jointing is spaced at 0.4 to 2.0 m (1.3 to 6.6 ft), and the joint trace length is seldom more than 3 m (10 ft). Joint surfaces are rough and do not contain any fill material. The bedding joints are poorly developed. Occasional prominent discontinuities with variable dip exist within the limestone formation. The UCS of this very strong limestone has been found to be up to 265 MPa (38,420 psi).

The pillars are square, 10.4 m (34 ft) wide and 8.2 m (27 ft) high on development. Room width was 13.4 to 14.6 m (44 to 48 ft). Benching was carried out, increasing the pillar height to 18.6 m (61 ft), which reduced the width-to-height ratio from 1.3 to 0.56. The depth of cover was approximately 90 m (300 ft). Several of the benched and partially benched pillars in this layout failed, while the development pillars are in good condition. Figure 10 shows one of the failed pillars at the edge of the benching operation. The pillar failed along two prominent discontinuities. The photograph was taken from the upper mining bench and does not show the full height of the

benched side of the pillar. The stress at failure of this pillar is estimated to be 14.4 MPa (2,080 psi) based on tributary area loading. However, using the Lunder-Pakalnis (1997) equation for pillar strength and a conservative value of the UCS at 200 MPa (29,000 psi), the benched pillars are predicted to have a strength of 64 MPa (9,280 psi), and one would not expect failure to occur.

The failure can, however, be explained by the weakening effect of the prominent discontinuities observed in the pillar. The discontinuities could have significantly reduced the strength of the benched pillar while having only a minor effect before benching, as predicted by the numerical models. This example demonstrates the importance of considering the potential effect of prominent discontinuities when designing slender pillars.

Conclusions

This evaluation of the strength of slender pillars has revealed the following:

- Empirical studies show that the strength of slender pillars is more variable than the strength of wider pillars. The increased variability implies that higher safety factors are required when designing slender pillars to account for the variability.

- Pillar-strength equations developed from empirical studies can predict significantly different strengths for slender pillars, even if identical rock strength values are used.

- Numerical models revealed that the process of brittle spalling and failure at low confinement plays an important role in the strength of slender pillars. The absence of a confined core causes failure to occur at the relatively low brittle strength of the rock.

- Numerical model results show that, for slender pillars, the difference between the pillar load at the onset of brittle spalling and the ultimate pillar strength can be small, implying that slender pillars are at or near the point of failure when they start to spall. This is not the case with wider pillars, where the ultimate strength can be much higher than the load required to initiate brittle spalling.

- Slender pillars are more sensitive to the presence of inclined discontinuities than wider pillars. Numerical models showed that relatively strong, inclined discontinuities can reduce the strength of slender pillars by as much as 70%, while wider pillars are affected to a much lesser degree. This sensitivity can partly explain the large variability in slender pillar strength seen in the results of published empirical pillar strength studies.

- The onset of brittle failure at relatively low stress and the significant reduction of slender pillar strength by prominent discontinuities have been observed in underground limestone mines.

Acknowledgments

The work presented in this paper forms part of the research program of the National Institute for Occupational Safety and Health in ground control and safety in underground mines. The contribution of Mr. John Ellenberger, who assisted in conducting the FLAC3D analyses, is gratefully acknowledged.

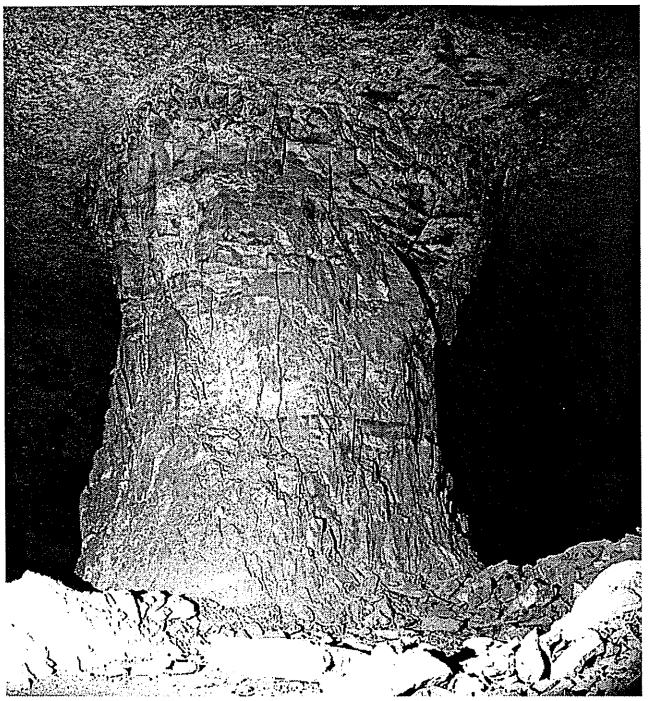

Figure 9 — A pillar with a width to height ratio of 0.77 showing the effect of brittle failure and spalling. Open vertical fractures/joints are visible in the pillar.

Figure 10 — Partially benched pillar that failed along two prominent discontinuities dipping at approximately 60°.

References

Anon., 2002, "FLAC 3D, Fast Lagrangian Analysis of Continua," User's Manual Version 2.1, Itasca Consulting Group, Minneapolis, Minnesota.

Barron, K. 1986, "A new method for coal pillar design" in *Conference on Ground Movement and Control Related To Coal Mining*, N. Aziz, ed., Aus. I.M.M. Melbourne, pp. 118-124.

Barton, N., and Choubey, V., 1977, "The shear strength of rock joints in theory and practice," *Rock Mechanics*, Vol. 10, pp. 1-54.

Brady, B.H.G., and Brown, E.T., 1985, *Rock Mechanics for Underground Mining*, George Allen and Unwin, London, 527 pp.

Bieniawski, Z.T., and van Heerden, W.L., 1975, "The significance of in-situ tests on large rock specimens," *Int. J. Rock Mech. & Min. Sci. & Geomech.*, Abstr., Vol. 12, pp. 101-103.

Diederichs, M.S., 2002, "Stress induced damage accumulation and implications for hard rock engineering," *NARMS-TAC 2002*, Hammah et al., eds., University of Toronto, pp. 3-12.

Diederichs, M.S., Coulson, A., Falmagne, V., Rizkalla, N., and Simser, B., 2002, "Application of rock damage limits to pillar analysis at Brunswick Mine," in *NARMS-TAC 2002*, Hammah et al., eds., University of Toronto, pp. 1325-1332.

Elmo, D., Coggan, J.S., and Pine, R.J., 2005, "Characterization of rock mass strength using a combination of discontinuity mapping and fracture mechanics modeling," in *40th US Rock Mechanics Symposium*, American Rock Mechanics Association, Anchorage, Alaska, Paper 05-733.

Esterhuizen, G.S., 2000, "Jointing effects on pillar strength," in *19th International Conf. on Ground Control in Mining*, Morgantown, West Virginia, University of West Virginia, pp. 286-290.

Gale, W.J., 1999, "Experience of field measurement and computer simulation methods of pillar design," *Second International Workshop on Coal Pillar Mechanics and Design*, National Institute for Occupational Safety and Health, IC 9448, pp. 49-61.

Hedley, D.G.F., and Grant, F., 1972, "Stope and pillar design for the Elliot Lake uranium mines," *Can. Inst. Min. Metall. Bull,*. Vol. 65, pp. 37-44.

Hoek, E. and Brown, E.T., 1980, *Underground Excavations in Rock*, Inst. Min. Metall., London.

Hoek, E., and Brown, E.T., 1997, "Practical estimates of rock mass strength," *Int. J. Rock Mech. & Min. Sci. & Geomech.*, Abstr., Vol. 34, pp. 1165-1186.

Iannacchione, A.T., 1999, "Analysis of pillar design practices and techniques for U.S. limestone mines," *Trans. Instn. Min. Metall.* (sect. A: Min. Industry), 108, September-December pp. A152-A160.

Kaiser, P.K., Diederichs, M.S., Martin, D.C., and Steiner, W., 2000, "Underground works in hard rock tunneling and mining," Keynote Lecture, *Geoeng2000*, Melbourne, Australia, Technomic Publishing Co., pp. 841-926.

Krauland, N., and Soder, P.E., 1987, "Determining pillar strength from pillar failure observations," *Eng. Min. Journal*, Vol. 8, pp. 34-40.

Lunder, P.J., 1994, "Hard Rock Pillar Strength Estimation an Applied Approach," M.A.Sc. Thesis, Dept. Mining and Mineral Process Engineering, University of British Columbia.

Lunder, P.J., and Pakalnis, R., 1997, "Determining the strength of hard rock mine pillars," *Bull. Can. Inst. Min. Metall.*, Vol. 90, pp. 51-55.

Mark, C., 1999, "Introduction to the proceedings," *Second International Workshop on Coal Pillar Mechanics and Design*, National Institute for Occupational Safety and Health, IC 9448, pp. 2-4.

Martin, C.D., and Maybee, W.G., 2000, "The strength of hard rock pillars," *Int. Jnl. Rock Mechanics and Min. Sci.*, Vol. 37, pp. 1239-1246.

Obert, L., and Duvall, W.I., 1967, "Rock mechanics and the design of structures," in *Rock*, Wiley, New York.

Potvin, Y., Hudyma, M., and Miller, H.D.S., 1989, "Rib pillar design in open stoping," *Can. Inst. Min. Metall. Bull.* Vol. 82, pp. 31-36.

Rojat, F, Labouise, V., Descoeudre, F., and Kaiser, P.K., 2003, "Lötschberg base tunnel: brittle failure phenomena encountered during excavation of the steg lateral adit," in *10th ISRM Congress*, South African Inst. Min Metall., pp. 927-933.

Salamon, M.D.G., and Munro, A.H., 1967, "A study of the strength of coal pillars," *J. South African Inst. Min. Metall.*, Vol. 68, pp. 55-67.

Stacey, T.R., and Yathavan, K., 2003, "Examples of fracturing of rock at very low stress levels," *ISRM 2003 Technology Roadmap for Rock Mechanics*, S. Afr. Inst. Min. Metall., pp. 1155-1159.

Von Kimmelman, M.R., Hyde, B., and Madgwick, R.J., 1984, "The use of computer applications at BCL Limited in planning pillar extraction and the design of mining layouts," In *Design and Performance of Underground Excavations, Int. Soc. Rock Mech. Symposium*, Brown and Hudson, eds., Brit. Geotech. Soc., London, pp. 53-63.

Wagner, H., 1974, "Determination of the complete load-deformation characteristics of coal pillars," in *3rd Congress, Int. Soc. Rock Mech.*, Denver, Colorado, VII, Part B, pp. 1067-1081.

Wagner, H., 1992, "Pillar design in South African collieries," in *Workshop on Coal Pillar Mechanics and Design*, U.S. Bureau of Mines, IC 9315, pp. 283-301.

Wilson, A.H., 1972, "An hypothesis concerning pillar stability," *The Mining Engineer*, Vol. 131, pp. 409-417.